Supplementary information

Distributed coding of stimulus magnitude across the rodent prefrontal cortex

Josephine Henke, David Bunk, Dina von Werder, Stefan Häusler, Virginia L Flanagin, Kay Thurley

Contents

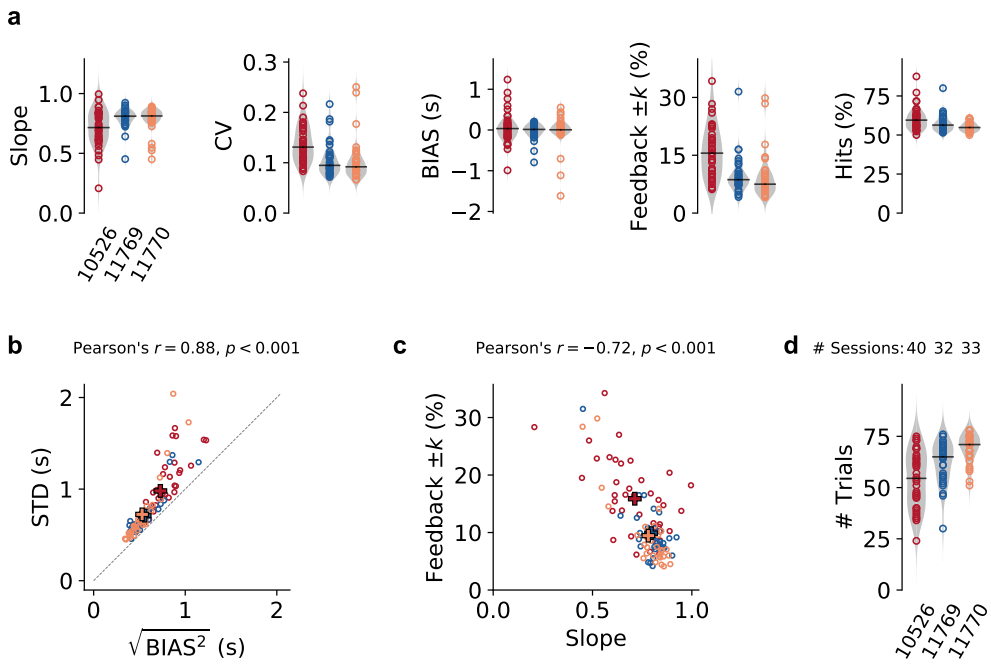

Figure S1. Behavioral characteristics. (a) Slope of the linear regression between stimuli and reproductions – quatifying the strength of the regression effect, with values closer to 1 meaning less regression –, coefficient of variation, bias, average tolerance k of the feedback range and percentage of hits for each animal. Values from single sessions are displayed as open circles. Color identifies individual animals. Violin plots illustrate the distribution of the population. A solid black line marks the median. Note that the slopes are consistently smaller than one, indicating the presence of the regression effect across sessions and animals. (b) The squared bias $\sqrt{\text{BIAS}^2}$ (quantifying systematic biases) and the standard deviation STD (quantifying overall variability) are correlated across animals and session. Note that the distance of each point from the origin of the coordinate system is the root-mean-square error, i.e. the Pythagorean sum of $\sqrt{\text{BIAS}^2}$ and standard deviation. Open circles correspond to single sessions. Crosses mark averages for an animal. Color-code as in (a). (c) Slope and feedback range are negatively correlated across animals and sessions, indicating wider feedback ranges for stronger regression effects. (d) Number of trials in each session.

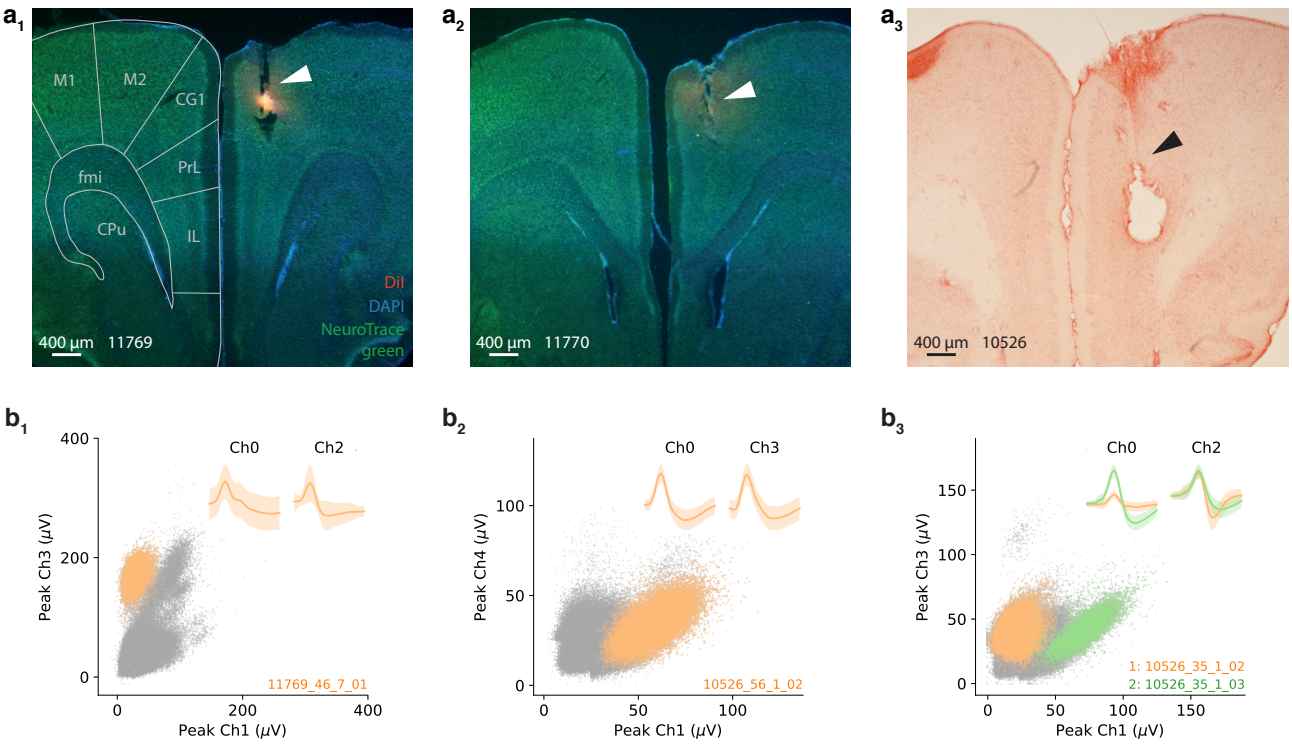

Figure S2. Electrophysiological recordings in gerbil mPFC – histology and spike sorting. (a) Representative coronal sections of the brains of all three gerbils. Tetrode tracks are visible in right cingulate cortex. In addition, stains from DiI coating of the tetrodes are visible in (a_1&a_2), and a big postmortem electrolytic lesion in (a_3). Background staining was done with DAPI and Neurotracer (a_1&a_2) and Neutralred (a_3). A section from a gerbil brain atlas is overlaid in (a_1) (Radtke-Schuller et al., 2016). M1, M2: primary and secondary motor cortex; Cg1: cingulate cortex, area 1; PrL: prelimbic cortex; IL: infralimbic cortex; fmi: forceps minor of corpus callosum; CPu: caudate putamen. (b) Spike clusters in feature space of mPFC cells recorded in three different sessions. (b_1) Cell from Fig. 2a in the main text. (b_2) cell from Fig. 2b in the main text. (b_3) cell from Fig. 2c (orange) in the main text and Fig. S4a (green). Peak signals are shown for two different channels of one tetrode as an example projection. Other spikes and voltage deflections are displayed as gray dots. *Insets:* average waveforms (1 ms length) corresponding to the colored clusters.

Example neurons

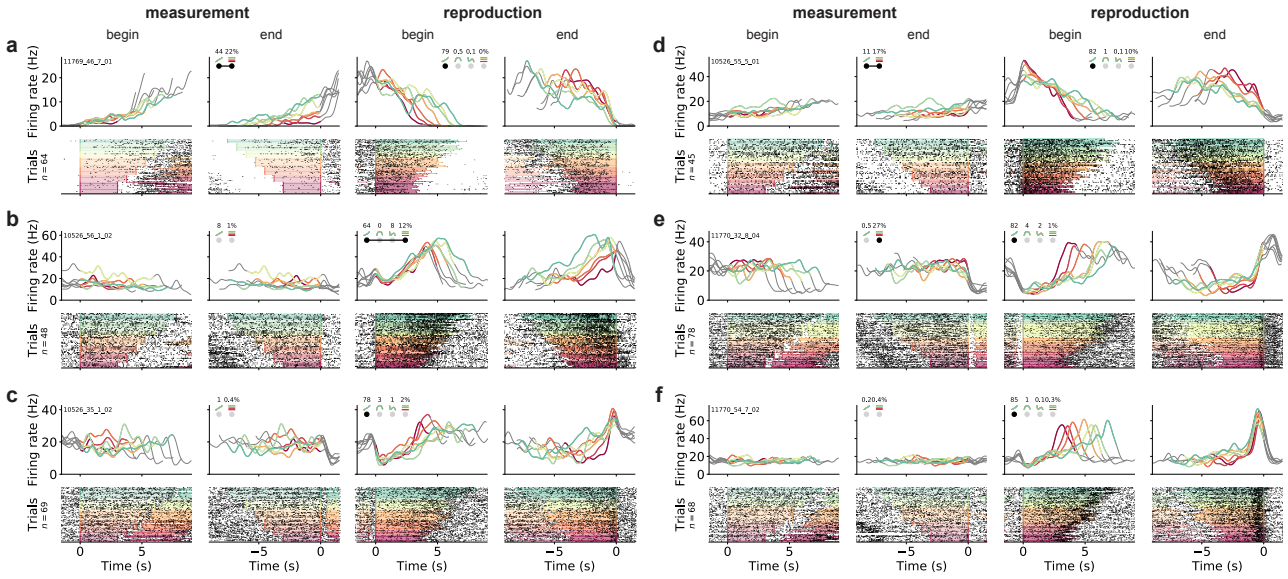

Figure S3. Ramping neurons. (a-c) Example cells from Fig. 2 in the main text. (d) Another cell that linearly increased its firing rate during measurement and ramped down to zero during reproduction. (e) A neuron that responded constantly but somewhat modulated by stimulus during measurement and ramps to threshold during reproduction. (f) Another ramp-to-threshold cell. (a-f) Panels display spike rasters sorted by stimulus (bottom) and corresponding spike density functions (SDF, top). Each column plots the data with different alignment, measurement begin and end, reproduction begin and end. Color identifies stimulus as in Fig. 1c. In the raster plots, black ticks are single spikes. For better visualization, we only plot half of the spikes (randomly chosen). Measurement or reproduction phases are delimited by underlayed color. The SDFs are colored in the respective task phase, outside they are displayed as thin gray lines. Markers in second and third panels show percent explained variance for each principal component. Black dots – that may be connected by a line – illustrate the cell type according to categorization (cf. Fig. 6a).

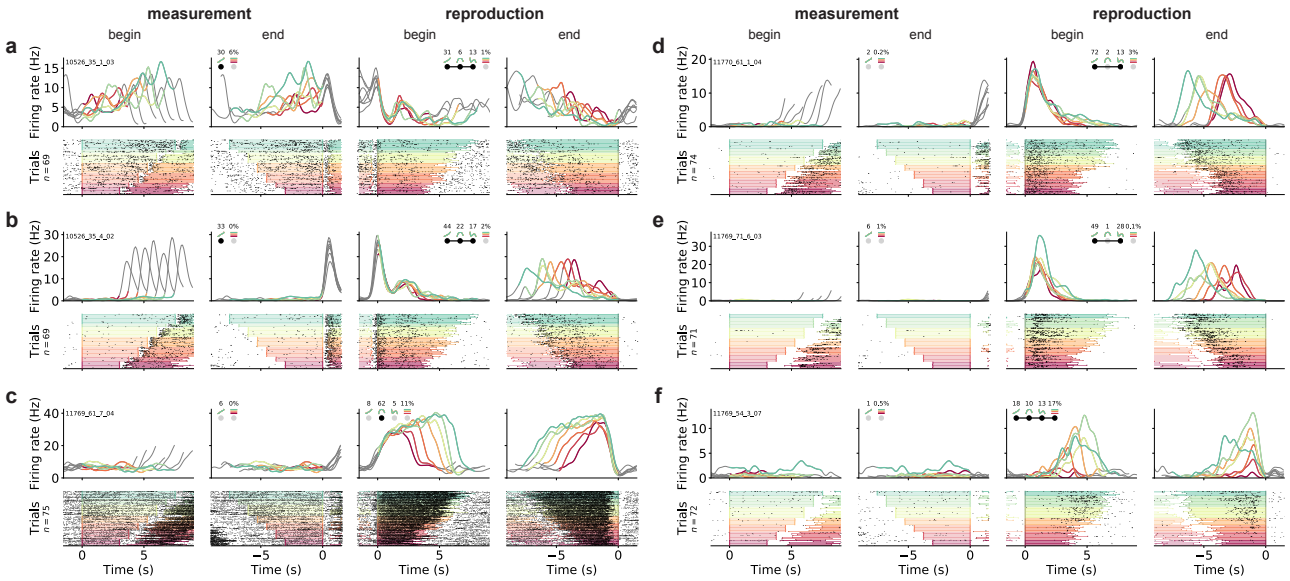

Figure S4. Absolute timing neurons. Examples of neurons that showed phasic responses at specific time points or for a certain duration in the reproduction phase. Plots are organized as in Fig. S3. Note, that the cell in (f) signals absolute time as it starts firing at 4 s – and proceeds until shortly before the end of the reproduced interval.

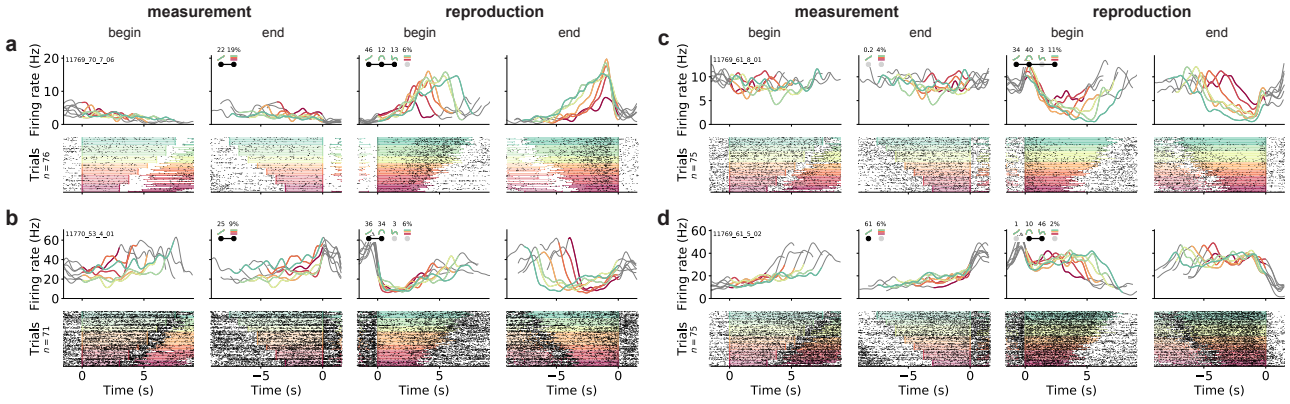

Figure S5. Other example neurons. Plots are organized as in Fig. S3. (a) A neuron that during reproduction appeared very similar to the cell in Fig. S4f, but in fact does not signal absolute but relative time as it starts firing later for longer stimuli. (b-d) Cells that during reproduction responded with brief (d) or extended drops of activity (c&d). The amount of activity reduction may (c) or may not (b) have scaled with the stimulus.

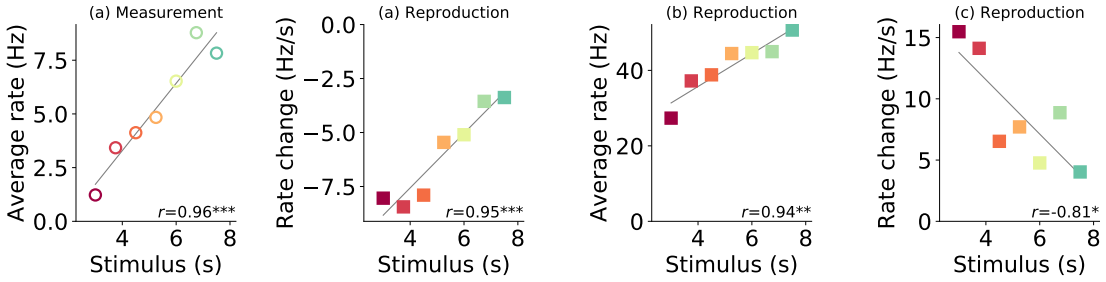

Figure S6. Firing of main text's example cells correlated with the stimulus duration. Single markers show the average firing rate or average change of firing rate at each stimulus interval during measurement or reproduction. Open dots are used for measurement and filled for reproduction. Solid lines are linear fits. On top of each panel the panel and task phase from Fig. 2 in the main text is indicated. In the lower right corner Pearson's correlation coefficient is given and significance is indicated. Average firing rate and average change of firing rate were calculated from the last half of the SDFs in the corresponding task phase.

Supplementary figures related to temporal scaling

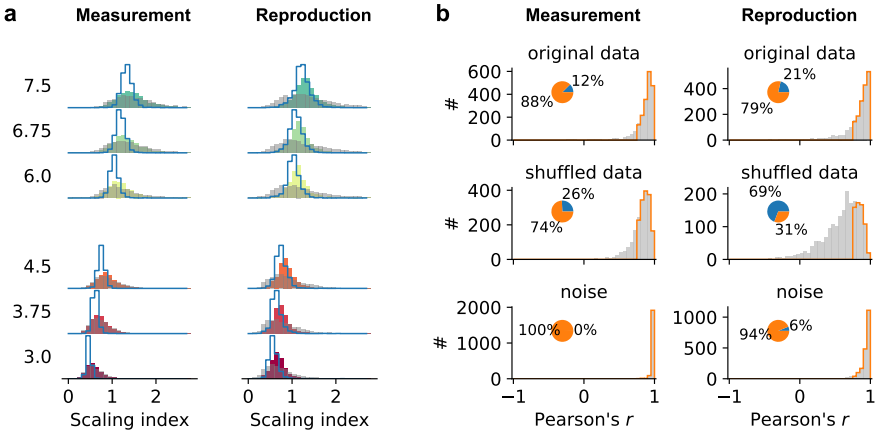

Figure S7. Temporal scaling for data, shuffled data and noise. (a) Distributions of scaling indices for all cells, i.e. center of mass of the SDF at every stimulus divided by the center of mass for 5.25 s (colored histograms; cf. Mello et al., 2015). In addition, panels contain distributions of scaling indices for shuffled data (grey histograms) and noise (blue outline). (b) Distributions of Pearson correlations of scaling indices with stimulus values (grey histograms). Significant values are delimited by an orange outline. Pie plots show significant (orange) and non-significant (blue) percentages. Large numbers of significant and positive correlations were present in the original data. Such high percentages are also found in shuffled data for measurement but not for reproduction, indicating that during reproduction scaling was explained by the neuronal activity. Values for noise surpassed those for data by far.

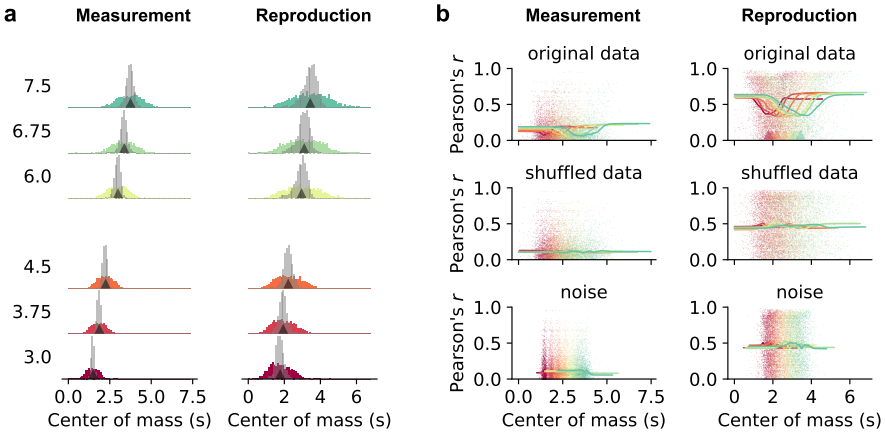

Figure S8. Neuronal activity but not noise tiles time intervals. (a) Distributions of center of mass for all cells (colored histograms). In addition, grey histograms give distributions of center of mass for noise. Arrow heads mark the middle of the stimulus interval or of the average reproduced interval. The actual neurons collectively tiled the time intervals during both measurement and reproduction. The center of mass for noise only covered the middle part of the whole time interval. (b) During reproduction, the average Pearson correlations of single cell activity for different stimuli (cf. Fig. 3f) were larger for neurons with center of mass at the begin and end of an interval. This suggests that neurons that scaled their activity had firing peaks at the border of the interval. Such a link did not exist for shuffled data and noise, and during measurement. Dots give single cell data and solid lines moving averages. Arrow heads in the upper right panel mark the middle of the average reproduced interval.

Supplementary figures related to principal component analysis

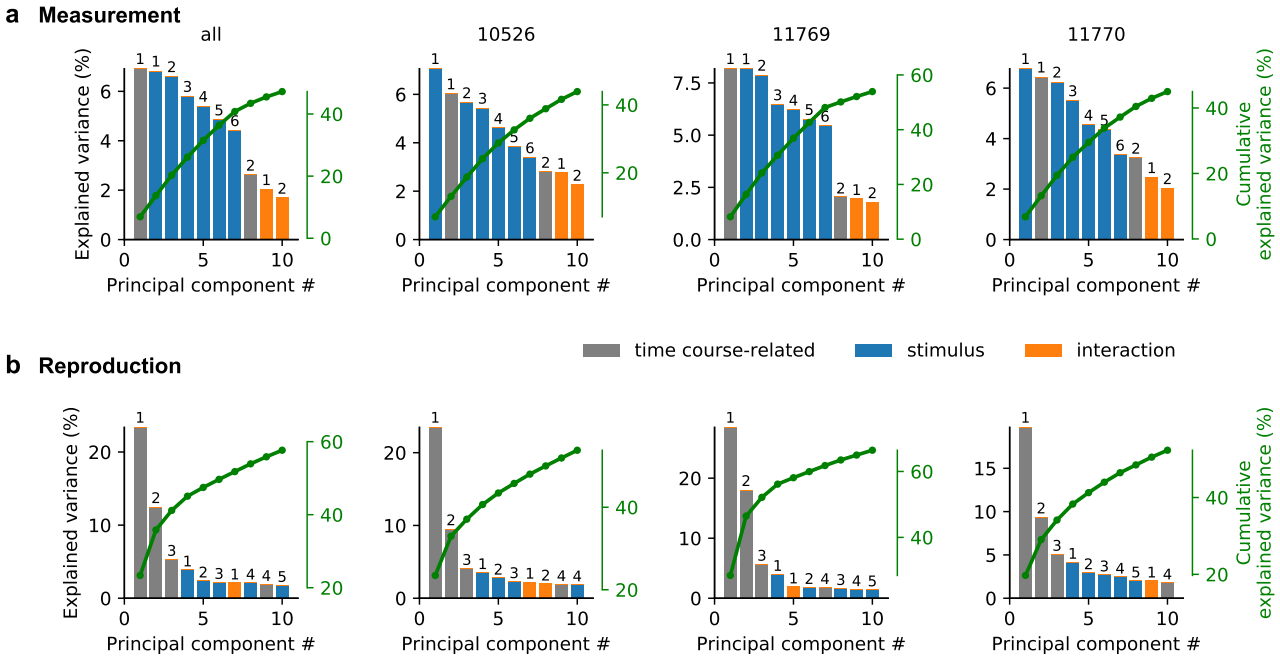

Figure S9. Explained variance of demixed PCA. Panels show explained variance for each principal component (bar graphs) and their cumulative explained variance (green line) of demixed PCA (Kobak et al., 2016) for measurement (a) and reproduction (b). Different panels correspond to all or individual animals. Numbers above bars give order with regard to component type, i.e. time course-related (gray), stimulus (blue), or interaction between both (orange). Results are comparable for individual animals and when pooled across all animals. In measurement the first time course-related and stimulus-dependent PCs are strongest. Reproduction is best explained by the first three time course-related PCs; only at forth place stimulus components start contributing.

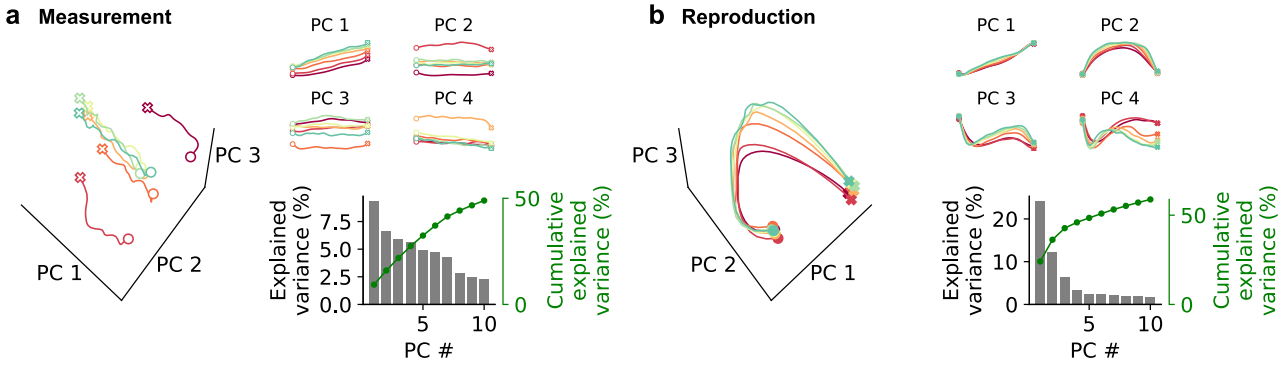

Figure S10. Decomposition with conventional principal component analysis. First four PCs for (a) measurement and (b) reproduction. Stimuli are colored as in other figures. Circles and crosses mark interval start and end. Open symbols are used for measurement and filled for reproduction. Bottom right panels: Explained variance for each principal component (bar graphs) and their cumulative explained variance (green line).

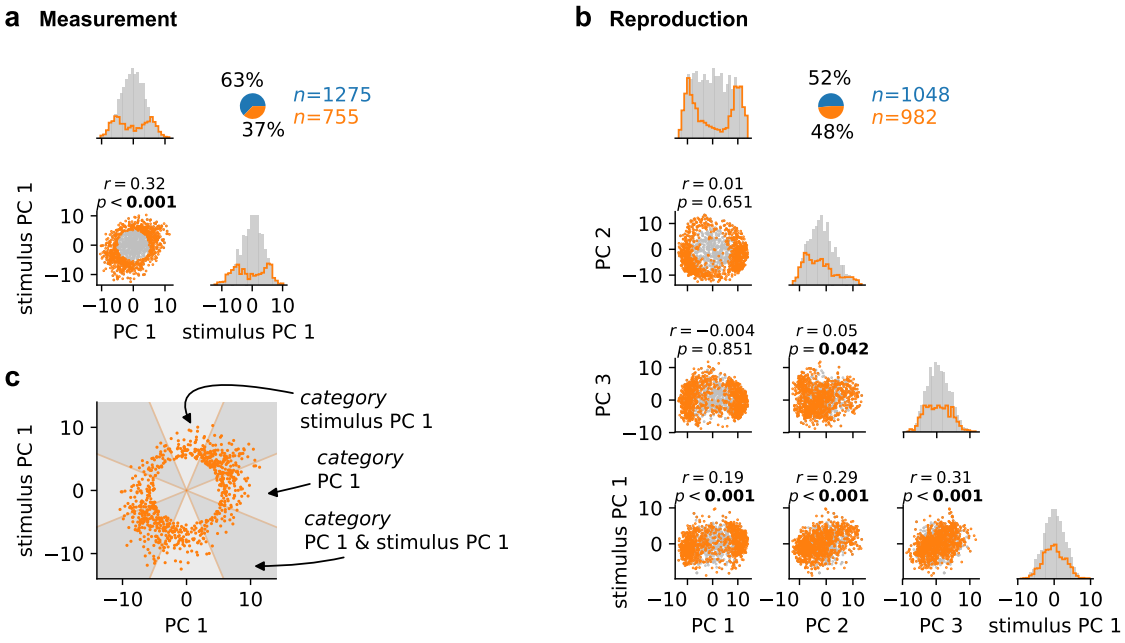

Figure S11. Distributions of and correlations between demixed PCA scores. (a) The scatter plot shows the correlation between scores for time course-related PC 1 and stimulus PC 1 in the measurement phase. Pearson's r and p-value are listed above the scatter plot. Both were calculated for all cells. Histograms give distributions for the PCs. Cells that can be explained by the two PCs are plotted in orange, all others in gray. Pie plot shows fractions of cells that can (orange) and can not (blue) be explained by the principal components. (b) Same as (a) for reproduction and for time course-related PCs 1-3 and stimulus PC 1. (c) Categorization procedure at the example of the measurement data in (a). Categories were determined only for cells that could be sufficiently explained by the PCs. Cells where counted as explained by a PC if the ratio of scores (in absolute values) to the other category was below $\tan(67.5°)$. For the measurement phase, this results in three different categories: PC 1 only, stimulus PC 1 only, or PC 1 + stimulus PC 1 illustrated by the three types of wedges in the plot.

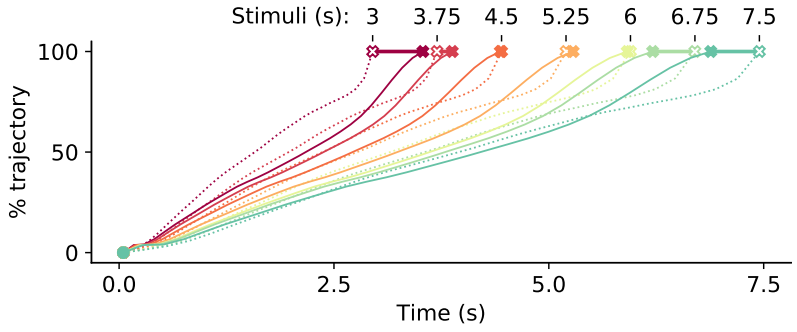

Figure S12. Population trajectory evolves at lower speeds for longer stimuli. The time course of PC 1 at each stimulus is plotted for measurement (dotted lines) and reproduction (solid lines). Stimuli are colored as in the other figures. Circles and crosses mark start and end of the trajectories. Open symbols are used for measurement and filled for reproduction. End points for same stimulus are connected by solid lines.

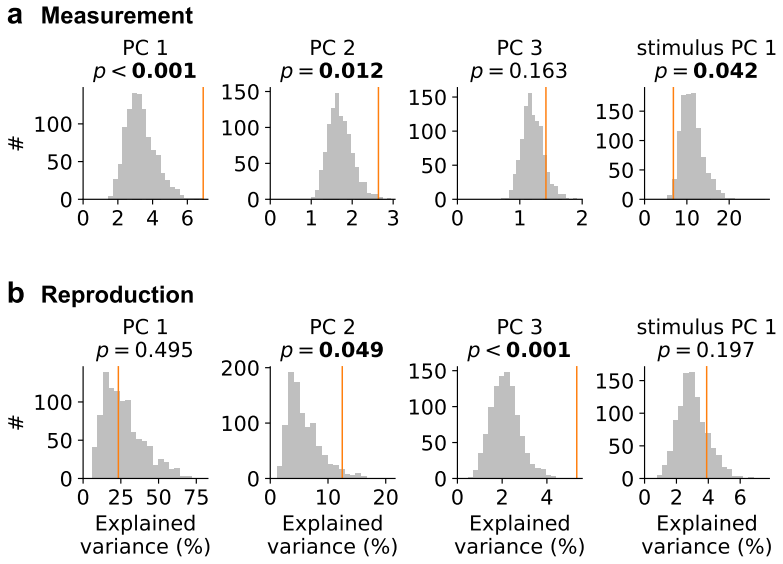

Figure S13. Collective activity adds to time course-related but not to stimulus-related PCs. We drew 1000 random tensor maximum entropy surrogate samples (Elsayed and Cunningham, 2017) for (a) measurement and (b) reproduction and determined the explained variance of time course-related components PC 1-3 and stimulus PC 1 (gray histograms). Orange vertical lines mark values for the original data. During measurement, PCs 1 and 2 for the original data were larger than expected. Similarly, PCs 2 and 3 were larger than expected during reproduction. Stimulus PC 1 was not different from expectation for reproduction and at the lower end of what was expected during measurement.

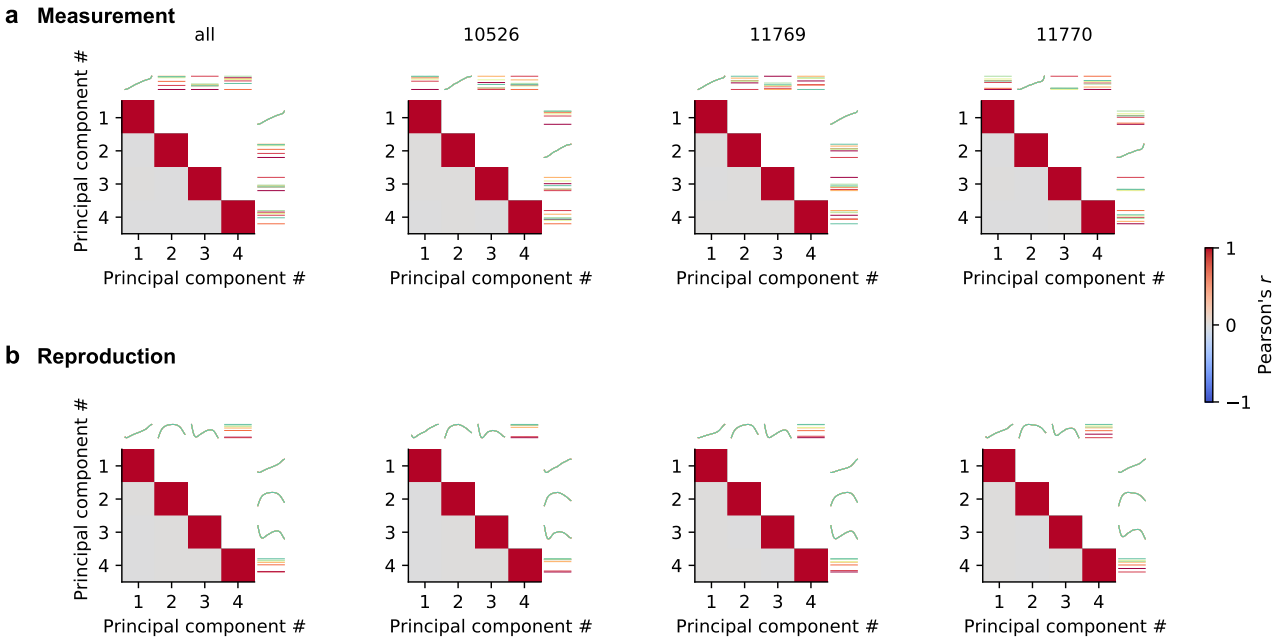

Figure S14. Proper demixing of principal components by demixed PCA. (a) Each panel shows correlations between all pairs of the first 4 demixed PCs for measurement. At top and to the left the principal components are illustrated. Different stimuli are color-coded as in other figures. Different panels give results for pooled data (all) and individual animals. (b) Same as (a) for reproduction. The correlations between different PCs are zero, indicating proper demixing.

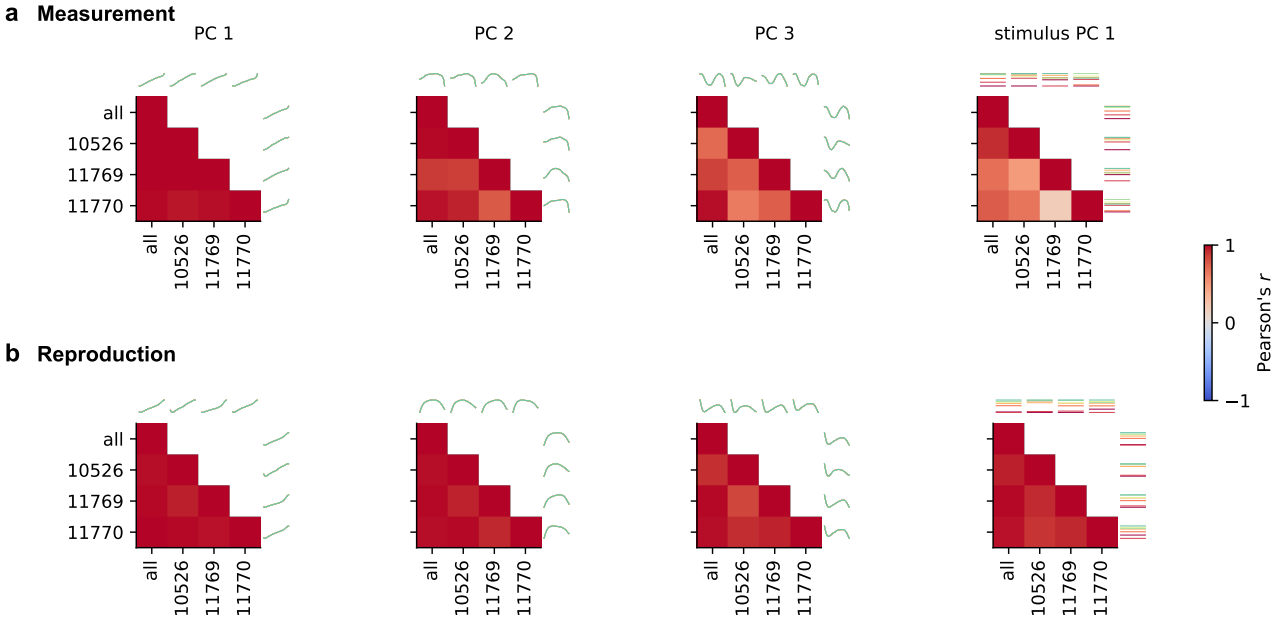

Figure S15. Demixed PCA results are similar for each animal. (a) Individual panels show correlations between all pairs of demixed PCs calculated for pooled data (all) and single animals for the measurement phase. At top and to the left the PCs are illustrated. Stimuli are color-coded. Different panels give time course-related PCs 1-3 and stimulus-related PC 1. (b) Same as (a) for reproduction. PCs are highly correlated across animals.

Supplementary figures related to time decoding

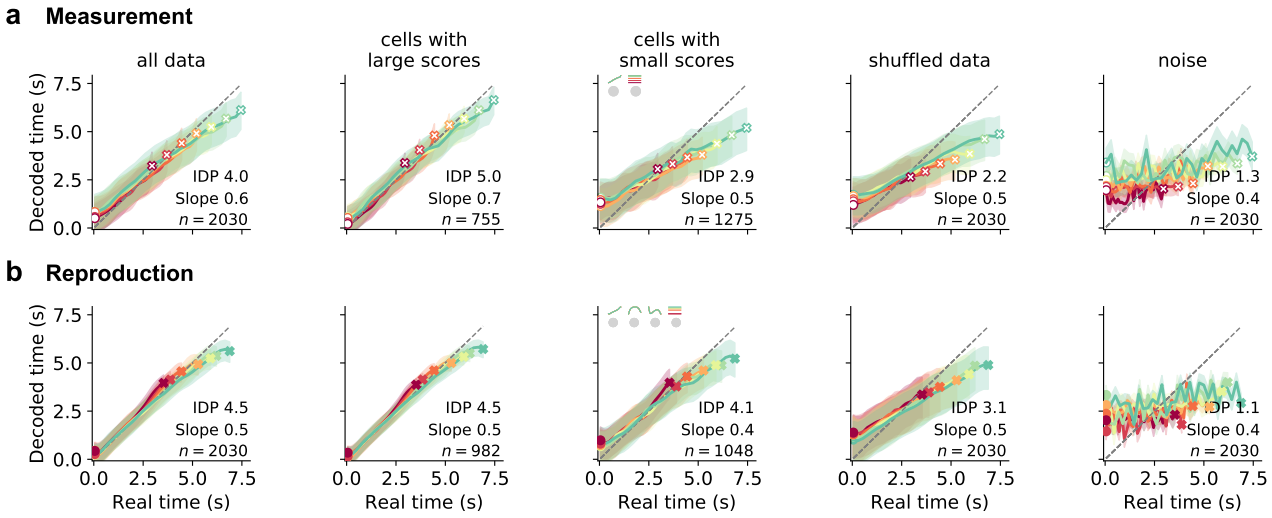

Figure S16. Decoding of elapsed time from data, shuffled data and noise. Decoded elapsed time from the whole population, cells with sufficiently large dPCA scores, cells with too small dPCA scores (cf. inset markers and Fig. 6 in the main text), shuffled data and noise for (a) measurement and (b) reproduction. Each panel displays decoded time vs. the real time for each stimulus (color-coded); average $\pm$ standard deviation (from bootstrapping). Circles and crosses mark start and end. Number of neurons, slope and indifference point of the final time values are given in lower right corner.

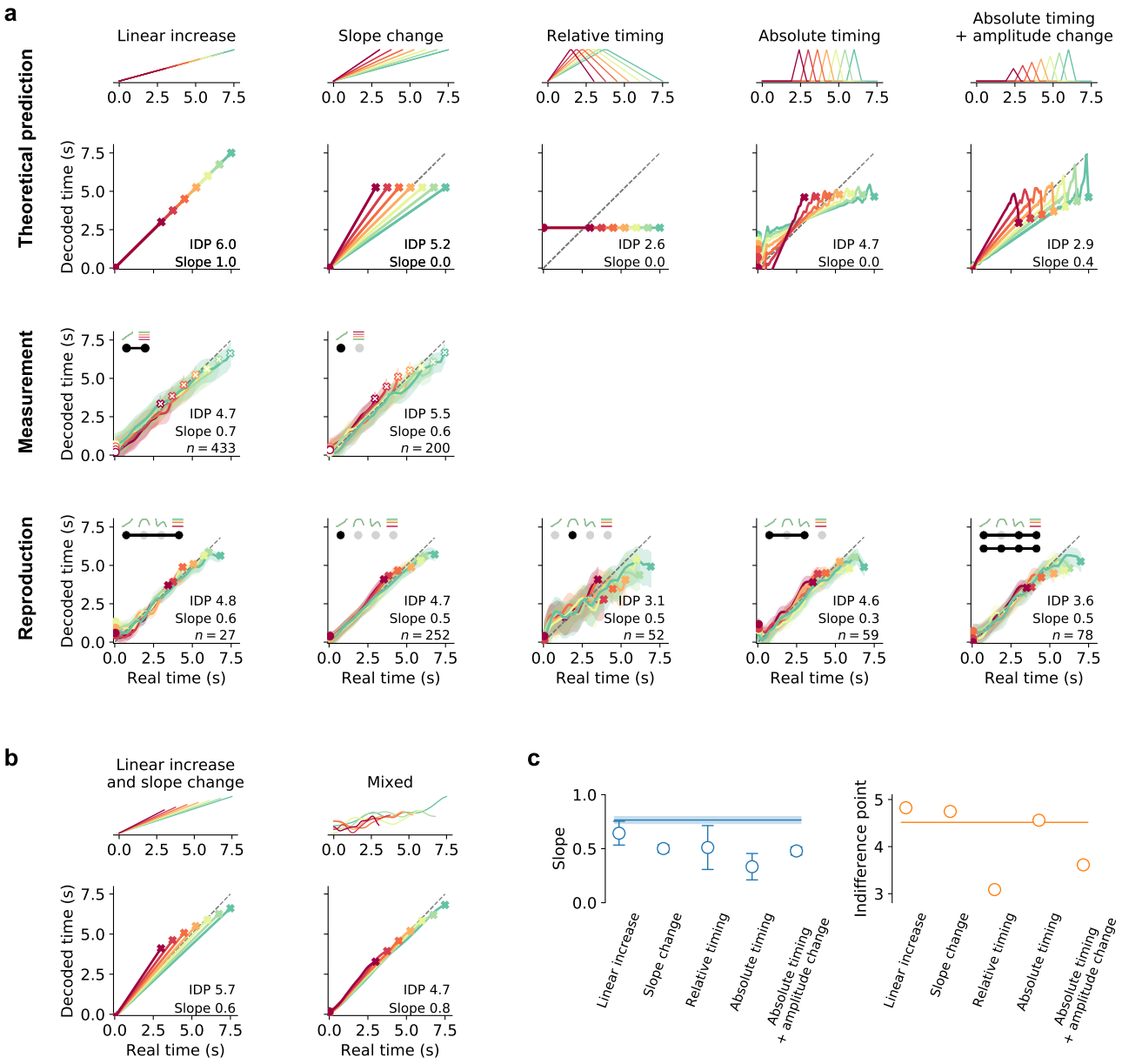

Figure S17. Response types encode elapsed time differently. (a) Different response types lead to different theoretical predictions when used for decoding elapsed time. Each column of panels corresponds to a different response type. The uppermost panel in each column displays example neuronal activity, the second panel from above shows the prediction for decoded time, and the third and forth panels plot the results for decoding from the neurons of the corresponding response type for measurement and reproduction, respectively. Average and standard deviation are derived from bootstrapping. Different stimulus intervals are color-coded. Circles and crosses mark start and end. Number of neurons, slope and indifference point of the final time values are given in lower right corner. Inset markers are according to Fig. 6 in the main text. (b) Mixtures of linear increasing activity and slope changes in (left) single neurons or (right) across the population (in the presence of noise, otherwise the linear regression fit and thus decoding would always be taken over by the neurons with linear increasing activity and no regression effect would be captured) explain behavioral regression effects. For the second case (right), a neuron with noisy linear increasing activity is provided as an example. (c) Slopes and indifference points of linear regression between final values of real and predicted time for the five response types during reproduction (lowest panels in a). Error bars are standard errors. Solid line and shading are average slope and standard error for the behavioral data.

References

Elsayed, G. F. and Cunningham, J. P. (2017). Structure in neural population recordings: an expected byproduct of simpler phenomena? *Nat Neurosci*, 20:1310–1318.

Kobak, D., Brendel, W., Constantinidis, C., Feierstein, C. E., Kepecs, A., Mainen, Z. F., Qi, X.-L., Romo, R., Uchida, N., and Machens, C. K. (2016). Demixed principal component analysis of neural population data. *eLife*, 5.

Mello, G. B. M., Soares, S., and Paton, J. J. (2015). A scalable population code for time in the striatum. *Curr Biol*, 25(9):1113–1122.

Radtke-Schuller, S., Schuller, G., Angenstein, F., Grosser, O. S., Goldschmidt, J., and Budinger, E. (2016). Brain atlas of the mongolian gerbil (meriones unguiculatus) in ct/mri-aided stereotaxic coordinates. *Brain Structure & Function*, 221 Suppl 1:1–272.